Anomalies in the NMR of silicon: Unexpected spin echoes in a dilute dipolar solid

A. E. Dementyev, D. Li, K. MacLean, and S. E. Barrett[1,*]
Department of Physics, Yale University, New Haven, Connecticut 06511, USA
(Received 26 June 2003; published 9 October 2003)

NMR spin echo measurements of ^{29}Si in silicon powders have uncovered a variety of surprising phenomena that appear to be independent of doping. These surprises include long tails and even-odd asymmetry in Carr-Purcell-Meiboom-Gill (CPMG) echo trains, and anomalous stimulated echoes with several peculiar characteristics. Given the simplicity of this spin system, these results, which to date defy explanation, present an interesting puzzle in solid state NMR.

DOI: 10.1103/PhysRevB.68.153302 PACS number(s): 72.25.Dc, 03.65.Yz, 03.67.Lx, 76.20.+q

In order to implement quantum computation (QC) based upon spins in semiconductors,[1–5] a detailed understanding of spin dynamics in these materials is required. To this end, we carried out a series of nuclear magnetic resonance (NMR) measurements that were motivated by a simple question: what is the ^{29}Si decoherence time (T_2) in silicon? Earlier NMR studies in silicon addressed other questions.[6–8]

We find that it is possible to detect the ^{29}Si [4.67% natural abundance (n.a.), spin-$\frac{1}{2}$] NMR signals out to much longer times than was previously thought possible, and so far, we have been unable to explain these results in terms of well-known NMR theory.[9] Surprises in such a simple spin system appear brand new to NMR, and understanding their origin is of fundamental importance. In this paper, we describe the phenomena and recount tests we have made to explore possible explanations.

Two standard experiments that measure T_2 are reported. First, using the Hahn echo sequence [HE: 90_X-(TE/2)-180_Y-(TE/2)-ECHO, where TE is a variable delay time (Ref. 10)], the measured decay, with $T_{2_{HE}} \approx 5.6$ ms, is in quantitative agreement with that expected for the static ^{29}Si-^{29}Si dipolar interaction. This decay mechanism is commonly encountered in solids, and a number of ingenious pulse sequences have been invented to manipulate the interaction Hamiltonian, pushing echoes out to times well beyond $T_{2_{HE}}$.[9,11–17] A common thread running through those sequences is the use of multiple 90° pulses, and pulses applied frequently compared to $T_{2_{HE}}$, which refocus the homonuclear dipolar coupling. The same cannot be said about the second sequence that we used to measure T_2, the Carr-Purcell-Meiboom-Gill sequence (CPMG: 90_X-{(TE/2)-180_Y-(TE/2)-ECHO}$^{\text{repeat } n \text{ times}}$ (Ref. 18)]. Specifically, the CPMG sequence is not expected to excite echoes beyond $T_{2_{HE}}$, since 180° pulses should not affect the bilinear homonuclear interaction. This statement is exact in two important limits: either for unlike spins or for magnetically equivalent spins.

Therefore, we were surprised to find that *CPMG echoes are detectable long after $T_{2_{HE}}$, and the echo peaks appear nearly identical in silicon samples with very different dopings.* This CPMG ''tail'' appears to be even larger at low temperatures. In addition, as the interpulse spacing (TE) is increased, the CPMG echoes develop a pronounced ''even-odd asymmetry'' [e.g., long after spin echo no. 1 (SE1) is in the noise, spin echo no. 2 (SE2) is clearly observable]. Lastly, we show how an ''anomalous stimulated echo'' is observed in this system, with several peculiar characteristics.

Figure 1 shows CPMG echo trains acquired in four different silicon samples (both *n* type and *p* type). As the legend shows, the ^{29}Si NMR spectrum [0.3 kHz$\leqslant$(FWHM)$\leqslant$3 kHz (FWHM denotes full width at half maximum)], the echo shape, and the T_1 [from 4.8 s to 5.5 h at room temperature (RT)] can be quite different, for samples with wide variations in doping.[19] Despite these big changes (e.g., $\times 10^6$ in *P* concentration), the peaks of the CPMG echoes are nearly identical to each other, and they persist long after the Hahn echoes have died away.

Qualitatively, the long tail evokes a well-known effect in liquid-state NMR, where diffusion causes slow changes in the local field leading to an extrinsic decay of the Hahn echoes.[9] Applying frequent refocusing pulses renders the dynamics ''quasistatic,'' enabling the CPMG echoes to persist to longer times, and revealing the intrinsic T_2. However, in

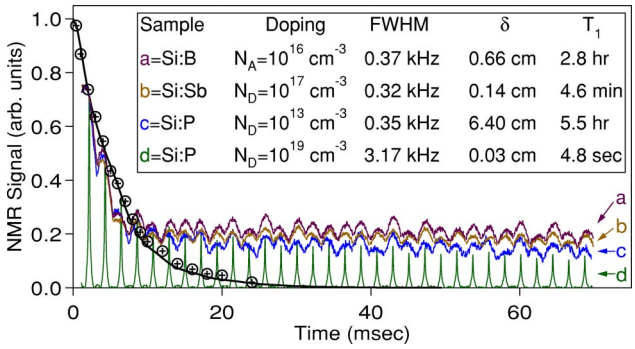

FIG. 1. (Color online) Two standard measurements of the ^{29}Si T_2 in powdered silicon at room temperature (RT). CPMG echo trains are shown for four samples (a–d) with different doping, full width at half maximum (FWHM), skin depth (δ), and spin-lattice relaxation time (T_1). Since samples *a*, *b*, and *c* exhibit much wider echoes than sample *d*; only the top portion of their echoes are visible. Hahn echo measurements (circles with crosses for sample *d*, others are suppressed for clarity) agree quantitatively with the dipolar decay curve (solid line) calculated for the silicon lattice [Eq. (4), see text]. Despite big changes in doping (e.g., $\times 10^6$ in P-concentration between samples *c* and *d*), the peaks of the CPMG echoes are nearly identical to each other, and they are detectable long after the Hahn echoes decay to zero. These measurements are in a 7.027 T field ($\vec{B} \| \hat{z}$, with $f_0 = 59.48$ MHz).

our data, the Hahn echoes appear to persist out to the "intrinsic" T_2 curve, *and the CPMG echoes are observed beyond even that limit*, as we now show.

A theoretical decay curve may be calculated and compared to the experiments in Fig. 1, starting from a general spin Hamiltonian for ^{29}Si in doped silicon. For example, for sample d, we have

$$\mathcal{H}=\mathcal{H}_{lab}+\mathcal{H}_{^{29}\mathrm{Si}\text{-}^{29}\mathrm{Si}}+\mathcal{H}_{^{29}\mathrm{Si}\text{-}^{31}\mathrm{P}}+\mathcal{H}_{^{29}\mathrm{Si}\text{-}e^-}, \tag{1}$$

where $\mathcal{H}_{lab}$ includes the magnetic coupling of ^{29}Si spins to both the static laboratory field and the time-dependent tipping field produced by the rf pulses. Since ^{29}Si is fairly dilute (4.67% n.a.), $\mathcal{H}_{^{29}\mathrm{Si}\text{-}^{29}\mathrm{Si}}$ is just the direct dipolar coupling. The last two terms, $\mathcal{H}_{^{29}\mathrm{Si}\text{-}^{31}\mathrm{P}}$ and $\mathcal{H}_{^{29}\mathrm{Si}\text{-}e^-}$, play the role of the "bath" for the ^{29}Si spins, which produce static magnetic shifts and determine T_1. In principle, the dynamics of this bath might also affect our T_2 measurements. However, Fig. 1 shows that this is not the case, since samples a–d have nearly identical CPMG tails despite very different baths. This is strong empirical evidence that the ^{29}Si homonuclear spin-spin coupling is sufficient to describe the physics of all four samples (a–d), which greatly simplifies the model. Therefore, in the rotating frame, the secular part of Eq. (1) (in the absence of rf pulses) is $\mathcal{H}_r$, given by[9]

$$\frac{\mathcal{H}_r}{\hbar}=\sum_i^{N_{spins}}\left(\Omega_i I_{z_i}+\sum_{j>i}^{N_{spins}}\{a_{ij}I_{z_i}I_{z_j}+b_{ij}(I_{x_i}I_{x_j}+I_{y_i}I_{y_j})\}\right), \tag{2}$$

where Ω_i is the magnetic shift for spin i (relative to on-resonance spins), $a_{ij}=[(^{29}\gamma)^2\hbar/r_{ij}^3][1-3\cos^2\theta_{ij}]$ ($^{29}\gamma$ is the gyromagnetic ratio for ^{29}Si), and $b_{ij}=-a_{ij}/2$. The vector between spins i and j, $\vec{r}_{ij}$, satisfies $\vec{r}_{ij}\cdot\hat{z}=r_{ij}\cos\theta_{ij}$.

If some of the terms in Eq. (2) are truncated, corresponding to specific physical limits, then analytic solutions for the effect of various pulse sequences may be found using the product operator formalism.[9,20] We start from the initial equilibrium density matrix:

$$\rho(t=0)\propto\sum_i^{N_{spins}} I_{z_i}, \tag{3}$$

which assumes the conventional strong field and high temperature approximations.[9]

For "unlike spins," where $|a_{ij}|\ll\Delta\Omega_{ij}\equiv|\Omega_i-\Omega_j|$, we truncate the b_{ij} terms.[9] In this limit, the peak of the kth CPMG echo decays according to

$$\langle I_Y(k\times\mathrm{TE})\rangle=\sum_i^{N_{spins}} I_{y_i}(0)\left\{\prod_{j>i}^{N_{spins}}\cos\left(\frac{a_{ij}(k\times\mathrm{TE})}{2}\right)\right\}, \tag{4}$$

which assumes the "infinite H_1 limit." Experimentally, $^{29}\gamma H_1/2\pi\approx 22$ kHz, $|a_{ij}/2\pi|<0.8$ kHz, $|\Omega_i/2\pi|<0.3$ kHz for samples a–c, and $|\Omega_i/2\pi|<3$ kHz for sample d. Equation (4) also describes a free induction decay (FID) following a single 90_X pulse in another limit: all the b_{ij} terms are truncated *and* all $\Omega_i=0$. Thus, the truncated dipolar decay of the CPMG echoes for the case of unlike spins is apparently unaffected by the 180_Y pulses, which flip all $I_{z_i}\rightarrow(-I_{zi})$, leaving the sign of the bilinear a_{ij} terms unchanged. In order to compare Eq. (4) to the data, we only need to have realistic values of a_{ij} for our powder samples. To obtain these a_{ij}, we built 20 000 "chunks" of the real silicon lattice with arbitrary orientations, and determined the ~80 nearest neighbors occupied according to the 4.67% n.a. Averaging Eq. (4) over all "chunks"[19] yields the solid curve shown in Fig. 1, which agrees remarkably well with the Hahn echo data points, but which fails to describe the measured CPMG echoes.

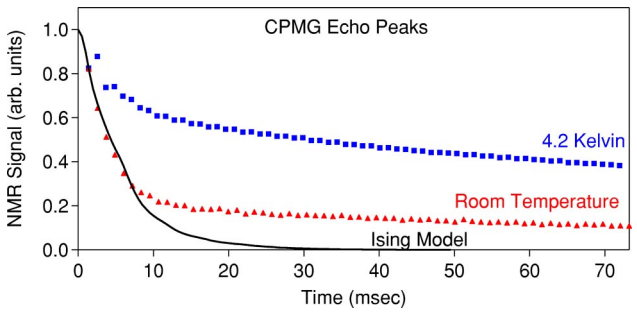

FIG. 2. (Color online) CPMG echo peaks at RT (triangles) and 4.2 K (squares) for sample *d*. The sets are scaled so that SE1 agree. The solid line is the calculated decay from Fig. 1 (see text). While the qualitative temperature effect is clear, the nonideal conditions of the 4.2 K data set (173_Y pulses and repetition time=100 s$\approx T_1/3$) prevent a quantitative assessment.

When CPMG experiments are carried out in liquids, the well-known echo modulation due to J coupling between unlike spins can be effectively turned off,[21] if pulses are applied so frequently that $1/\mathrm{TE}\gg J_{ij}$ and $1/\mathrm{TE}\gg\Delta\Omega_{ij}$. Similarly, in our solid-state measurements, applying a CPMG sequence with frequent pulses (i.e., small TE) might push the system artificially into the "like spin" regime, where $|a_{ij}|\gg\Delta\Omega_{ij}$. In that limit, all the terms of Eq. (2) should be retained. This precludes an analytic solution, but numerical calculations of $\langle I_Y(t)\rangle$ can be carried out for small numbers of spins, including the required ensemble averaging.[19] These calculations show that the initial decay of the CPMG echoes in that limit should be $\approx\frac{2}{3}$ *faster* than Eq. (4), which agrees with the well-known second moment expressions.[9,22] Our data require another explanation.

Empirically, the long tail induced by the CPMG sequence has several interesting characteristics.[19] For example, Fig. 2 shows that the tail height, relative to the first echo, grows as the sample is cooled down to 4.2 K. This result is only qualitative, since the tail height can also be changed by using a repetition time $<T_1$ and by using tip angles slightly away from 180°, which can be difficult to avoid at $T=4.2$ K. Still, even taking these factors into account, the tail appears to be more pronounced at low temperatures.[19]

To see if the long tail was due to some kind of multiple-pulse spin locking, we increased the interpulse spacing (TE), which led to another unexpected result. Figure 3(a–c) shows data taken at 4.2 K for three different TE in sample *d*. The long tail persists even for $\mathrm{TE}>T_{2_{HE}}$. Interestingly, for large interpulse spacings, the odd-numbered echoes are much

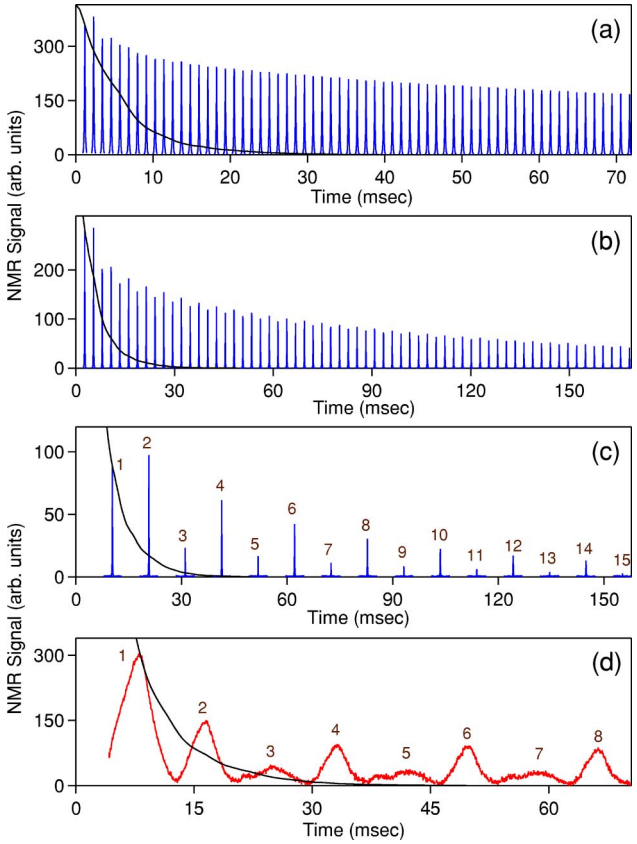

FIG. 3. (Color online) CPMG echo trains at 4.2 K for sample d with TE of (a) 1.12 ms, (b) 2.65 ms, and (c) 11.23 ms. The solid line from Fig. 1 is scaled to intercept the first echo in each graph. The numbered echoes in (c–d) exhibit a pronounced even-odd asymmetry, which emerges for TE $>T_{2_{HE}}$. (d) shows the same effect in Si:Sb at RT with well-calibrated pulse angles, low repetition rates, and a narrow spectrum.

smaller than the even-numbered echoes. At RT, samples *a*–*d* exhibit the same even-odd asymmetry as TE is increased [e.g., as in Fig. 3(d)].

This even-odd asymmetry leads to remarkable results as TE is increased still further. Figure 4 shows the FID and first two spin echoes acquired in a CPMG experiment with $n=2$, for very long TE. In Fig. 4(a) $\mathrm{TE}/T_{2_{HE}}\approx 5.35$ so that SE1 is tiny relative to the FID. Surprisingly, SE2 (at $2\times\mathrm{TE}/T_{2_{HE}}\approx 10.7$) is nearly three times the height of SE1; SE2 is also narrower than SE1. In Fig. 4(b), TE is doubled, which pushes SE1 into the noise, while SE2 is clearly visible, *even though it occurs* $21.4T_{2_{HE}}$ *after the* 90_X *pulse*.

Since SE2 is the first echo to occur after three pulses, we decided to look for a contribution to the CPMG echoes that is reminiscent of a stimulated echo,[10] using the sequence 90_X-(TE/2)-180_Y-TM-180_Y-DETECT, where delay times TE and TM can be varied independently. Using this sequence, we detect a conventional spin echo SE2 that peaks at total time $2\times$TM, along with an ''anomalous stimulated echo'' (STE_A) that peaks at TM+TE. Figure 5 shows the height of the STE_A as either TM or TE is varied. There are several remarkable features of the data in Fig. 5: (1) we observe

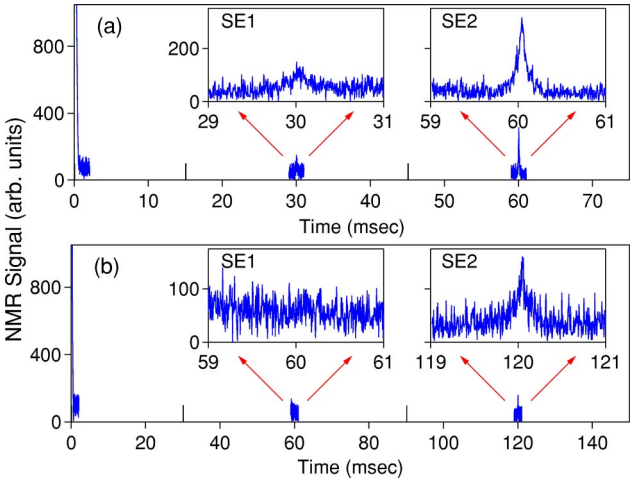

FIG. 4. (Color online) The free induction decay (FID) and first two spin echoes (SE1, SE2) excited by a CPMG sequence at RT for sample *d* with TE of (a) 30 ms and (b) 60 ms. The insets show the narrow shape and the height of SE2 in comparison with SE1 (the FID starts at 14 600). At 60 ms, SE2 (a) is clearly different from SE1 (b). Solid bars indicate pulses.

STE_A, even for our best 180_Y pulses, where there should be none, (2) they decay slowly as TE or TM are increased, (3) they appear to ''start'' at nonzero values at the left edge of Fig. 5, and (4) the data set has a larger scatter than expected, given the signal to noise of each individual data point.

Given the results in Figs. 1–5, we have tried to minimize the effects of nonidealities commonly reported in multiple pulse NMR:[9,16,17] (i) inhomogeneous H_1, (ii) finite-size H_1, (iii) a ''spin locking'' effect, and (iv) phase transients.[16] For (i), the results are unchanged if we use a tiny ($\sim$6%) coil filling factor, or samples of very different skin depths. For (ii), the same effects are seen in all samples, even though $H_1/(\mathrm{FWHM})$ changes by a factor of 10. For (iii), similar results are obtained with an alternating phase Carr-Purcell sequence, where 180° pulse phases alternate between $-X$ and X, even though the average H_1 is quite different from that of CPMG. Finally, we expect that (iv) becomes less important as the number of pulses is reduced and their spac-

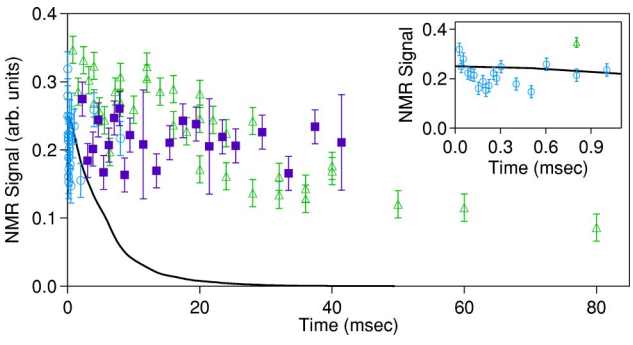

FIG. 5. (Color online) ''Anomalous stimulated echo'' amplitudes at RT for sample *d*. Filled squares (TE$\approx$0.4 ms) are plotted vs TE+TM. Empty circles (TM$\approx$10 ms) and triangles (TM $\approx$21 ms) are plotted vs TE. The solid line is from Fig. 1. Inset: The signal does not appear to grow from zero.

ing is increased, so we do not see how this could explain the puzzling results of Figs. 4 and 5.

Taken together, these results strongly suggest that the effects are due principally to the ^{29}Si homonuclear dipolar coupling. In that case, why is it so hard to find a quantitative explanation for the data? The form of Eq. (2) for a clean silicon sample is one problem, since many spins may have $|a_{ij}| \sim \Delta\Omega_{ij}$, which make simulations[19] particularly challenging.[23] The dilution of the moments on the lattice could be another issue.[24] The strange features in Fig. 5 (in particular, point 3), and the narrowness of SE2 in Fig. 4 seem to be beyond the conventional theory of solid-state NMR. In recent NMR experiments,[25] large polarizations have produced measurable dipolar field effects, which led some to question the approximations underlying Eq. (3). While we do not have such large polarizations, the effects do appear to be more pronounced at low temperatures (Fig. 2).

In the broader context of QC, the generic form of Eq. (2) suggests that similar surprises may be found in other systems with small, long-range, qubit-qubit interactions, particularly when ''bang-bang'' control is used.[26] Understanding these phenomena in silicon may help to prevent similar surprises from imposing a performance limit on quantum computers in the future.

This work was supported by the National Security Agency (NSA) and Advanced Research and Development Activity (ARDA) under Army Research Office (ARO) Contract No. DAAD19-01-1-0507 and DAAD19-02-1-0203. We would like to thank T.P. Ma (Yale EE) for providing the Si:P samples, and also R. Falster (MEMC) for providing the Si:B and Si:Sb samples that were used in this study. We thank C.P. Slichter, R. Tycko, W.S. Warren, D.G. Cory, T.F. Havel, J.S. Waugh, R.G. Griffin, S.M. Girvin, A. Vestergren, and V.V. Dobrovitski for stimulating discussions. In particular, we appreciate the help of K.W. Zilm and X. Wu, who independently verified several of these results.

*Email address: sean.barrett@yale.edu

[1] B.E. Kane, Nature (London) **393**, 133 (1998); Fortschr. Phys. **48**, 1023 (2000).
[2] V. Privman, I.D. Vagner, and G. Kiventsel, Phys. Lett. A **239**, 141 (1998).
[3] D.P. DiVincenzo and D. Loss, J. Magn. Magn. Mater. **200**, 202 (1999).
[4] R. Vrijen, E. Yablonovitch, K. Wang, H.W. Jiang, A. Balandin, V. Roychowdhury, T. Mor, and D. DiVincenzo, Phys. Rev. A **62**, 012306 (2000).
[5] T.D. Ladd, J.R. Goldman, F. Yamaguchi, Y. Yamamoto, E. Abe, and K.M. Itoh, Phys. Rev. Lett. **89**, 017901 (2002).
[6] R.G. Shulman and B.J. Wyluda, Phys. Rev. **103**, 1127 (1956).
[7] G. Lampel, Phys. Rev. Lett. **20**, 491 (1968).
[8] R.K. Sundfors and D.F. Holcomb, Phys. Rev. **136**, A810 (1964); H. Alloul and P. Dellouve, Phys. Rev. Lett. **59**, 578 (1987); S.E. Fuller, E.M. Meintjes, and W.W. Warren, *ibid.* **76**, 2806 (1996).
[9] C.P. Slichter, *Principles of Magnetic Resonance*, 3rd ed. (Springer, New York, 1990).
[10] E.L. Hahn, Phys. Rev. **80**, 580 (1950).
[11] J.G. Powles and P. Mansfield, Phys. Lett. **2**, 58 (1962).
[12] E.D. Ostroff and J.S. Waugh, Phys. Rev. Lett. **16**, 1097 (1966).
[13] W.K. Rhim, A. Pines, and J.S. Waugh, Phys. Rev. Lett. **25**, 218 (1970); Phys. Rev. B **3**, 684 (1971).
[14] J.S. Waugh, L.M. Huber, and U. Haeberlen, Phys. Rev. Lett. **20**, 180 (1968).
[15] P. Mansfield, J. Phys. C **4**, 1444 (1971); W.K. Rhim, D.D. Elleman, and R. W. Vaughan, J. Chem. Phys. **58**, 1772 (1973).
[16] U. Haeberlen, *High Resolution NMR in Solids: Selective Averaging*, Supplement 1 to *Advances in Magnetic Resonance* (Academic Press, New York, 1976).
[17] M. Mehring, *High Resolution NMR in Solids*, 2nd ed. (Springer-Verlag, Berlin, 1983).
[18] H.Y. Carr and E.M. Purcell, Phys. Rev. **94**, 630 (1954); S. Meiboom and D. Gill, Rev. Sci. Instrum. **29**, 6881 (1958).
[19] D. Li, A.E. Dementyev, K. MacLean, and S.E. Barrett (unpublished).
[20] O.W. Sorensen, G.W. Eich, M.H. Levitt, G. Bodenhausen, and R.R. Ernst, Prog. Nucl. Magn. Reson. Spectrosc. **16**, 163 (1983).
[21] R. Freeman, *Spin Choreography: Basic Steps in High Resolution NMR* (Oxford University Press, Oxford, 1998).
[22] J.H. Van Vleck, Phys. Rev. **74**, 1168 (1948).
[23] A. Allerhand, J. Chem. Phys. **44**, 1 (1966).
[24] E.D. Fel'dman and S. Lacelle, J. Chem. Phys. **104**, 2000 (1996); S. Lacelle and L. Tremblay, *ibid.* **102**, 947 (1995).
[25] W.S. Warren, W. Richter, A.H. Andreotti, and B.T. Farmer, Science **262**, 133 (1993); S. Lee, W. Richter, S. Vathyam, and W.S. Warren, J. Chem. Phys. **105**, 874 (1996).
[26] L. Viola and S. Lloyd, Phys. Rev. A **58**, 2733 (1998).